

A PROJECT REPORT ENTITLED

SELECTIVE LASER MELTING PROCESS OF Ti6Al4V (ASTM GRADE-5) POWDERS USING COMSOL SOFTWARE

Submitted for fulfilment of the requirement of Midterm Evaluation of the course on
Modern Manufacturing Methods (MAE 545)

Submitted by:

SHERRY DANIEL SAJAN

ASU ID: 1225838460

Guided by:

PROF. QIONG NIAN



Spring Semester 2023

Department of Mechanical & Aerospace Engineering,

School for Engineering of Matter, Transport and Energy (SEMTE)

Arizona State University, Tempe, AZ, 85281

TABLE OF CONTENTS

1. ABSTRACT-----	4
2. INTRODUCTION-----	4
3. MODELING AND ANALYSIS OF POWDER BED-----	5
a. 3-D Block Geometry-----	5
b. Parameters used for simulation-----	5
c. Assigning the Major Variables-----	6
d. Creating Custom Ti6Al4V material-----	6
e. Assigning Layered Material-----	7
f. Defining the Laser heat source-----	8
g. Defining Convection Heat flux-----	8
h. Defining Radiation-----	9
i. Defining Bed temperature-----	9
j. Setting up Mesh for the powder block-----	10
k. Solver Settings-----	10
4. RESULTS AND DISCUSSION-----	11
a. Laser Travel Illustration-----	11
b. Defining a cut plane-----	11
c. Melt pool-----	12
d. Temperature distribution of powder with Time-----	14
e. Temperature variation in changing Laser Parameters-----	16
5. CONCLUSION-----	18
6. REFERENCES-----	18

LIST OF FIGURES

Figure 1- Ti6Al4V Powder Block-----	5
Figure 2- Adding Material Parameter function-----	7
Figure 3- 3 Layer Material -----	7
Figure 4- Selecting the center domain for Laser Heat source-----	8
Figure 5- Selecting domains for Convection and Radiation -----	9
Figure 6- Selecting Bottom domain of the block for bed temperature-----	9
Figure 7- Setting up Mesh for Block-----	10
Figure 8- Simulation Solver Setting -----	10
Figure 9- Laser travel on the block at different time interval-----	11
Figure 10- Defining Cut plane ZX (Left) and YZ(Right) -----	11
Figure 11- Cut view (ZX) of Ti6Al4V Block in 3D -----	12
Figure 12- Cut view (ZX) of Ti6Al4V block in 2D displaying Melt pool -----	12
Figure 13- Cut view (YZ) of Ti6Al4V showing melt pool and temperature distribution at different time intervals-----	13
Figure 14- Temperature Distribution with time using Domain probe -----	14
Figure 15- Selecting Laser path edges for Edge probe -----	14
Figure 16- Temperature Distribution with time using Edge probe-----	15
Figure 17- Selecting a point for Boundary point probe-----	15
Figure 18- Temperature Distribution with time using Boundary Point probe -----	15
Figure 19- Temperature Variation by varying the Scan speed: (a) $V_s = 3\text{mm/s}$, (b) $V_s = 10\text{mm/s}$ -----	16
Figure 20- Temperature Variation by Varying Energy Density: (a) $E_d = 8.84\text{E}+06$, (b) $E_d = 1.24\text{E}+07$, (c) $E_d = 2.12\text{E}+07$ -----	17

LIST OF TABLES

Table 1- Parameters used for Simulation-----	6
Table 2- Major Variables used for Simulation-----	6
Table 3- Material Properties for Custom Ti6Al4V-----	7
Table 4- Layered Material Settings -----	8
Table 5- Temperature Variation with Varying Laser Scan Speed -----	16
Table 6- Temperature Variation with Varying Laser Energy Density-----	17

1. ABSTRACT

The research community has recently given selective laser melting (SLM) a great deal of attention due to the viability of creating customized complicated metallic structures with applications in the medicine, aviation, and energy industries. One of the most popular and promising areas is the SLM of Ti6Al4V powders.

In this report, the concept and procedure for laser powder bed fusion (also known as selective laser melting), a technology that is frequently employed in additive manufacturing, are introduced. In order to explore the laser heating of a solid Ti6Al4V powder bed, a simple finite element model was created using COMSOL Multiphysics Software. The simulation is Time dependent study. Nd-YAG laser parameters is used.

After the results of the simulation were analyzed, steps such as defining the melting pool and plotting the temperature history/evolution of various locations in the powder bed and temperature increase/decrease as a function of time were taken to determine the melting pool's size from a cross-sectional view. Also, by varying the Laser scan speed as well as Energy density, the temperature distribution with time was also analyzed.

Index terms: Additive Manufacturing, Melt Pool, Selective Laser Melting, COMSOL

2. INTRODUCTION

The phrase "additive manufacturing" (ASTM F2792) is used by the industry to refer to all of the technology's uses. In contrast to subtractive manufacturing methods, it is defined as the process of combining materials to create items from 3D model data, typically layer by layer. Freeform fabrication, additive layer manufacturing, additive procedures, and additive techniques are all synonyms for this process.

Among the most popular powder bed fusion-based additive manufacturing (AM) technologies is selective laser melting (SLM). Early this century, various businesses, including EOS GmbH, Concept Laser GmbH, MTT Technologies, etc. successfully demonstrated this technology before making it commercially available. The improvement of build size, speed, and material compatibility has been the main focus of extending the capability of commercialized SLM machines. Large build platforms for SLM machines have been introduced by EOS, Concept Laser, and SLM Solutions. Examples include the EOS M400, Concept Laser X-line 1000R (X-axis up to 630 millimeters), and SLM 500HL.

The time it takes to create a part can be significantly decreased by increasing layer thickness and recoating speed. SLM can be used with a growing variety of metallic powders, including stainless steels, tool steels, and biocompatible alloys like Titanium alloys. The ASTM grade-5 material Ti6Al4V has exceptional corrosion resistance and a good strength-to-weight ratio. Extra low interstitial Ti6Al4V (ASTM grade 23) has been developed with increased ductility and fracture toughness and lower amounts of oxygen, nitrogen, carbon, and hydrogen. Moreover, the SLM/LPBF process has a number of benefits, including increased functionality, near-net-shape fabrication with little to no post-processing, faster lead times, free complexity, etc. The SLM method has uses in the automotive, jewelry, food, oil refinery, marine, aerospace, and automobile industries, among others. However, there are certain issues with the SLM sector, including (a) alloy creation based on SLM, (b) early failure of materials despite observable improvements in their properties, (c) process development and innovation, (d) numerical simulations, etc.

3. MODELING AND ANALYSIS OF POWDER BED-

a. 3-D Block Geometry-

A rectangular porous Ti6Al4V metal block is taken into consideration for the simulation procedure in accordance with the Selective laser melting technique as depicted in fig. This is a custom-made material with the Layered Material property in COMSOL (3 layers of alternate Ti6Al4V and air) to make it porous structure and then assigned it to the block.

A block is created with dimensions of 3.6 mm in length, 1.2 mm in width, and 0.5 mm in height. In order for the laser beam to be assigned to travel on the top center layer, it is separated into three layers as shown in the figure.

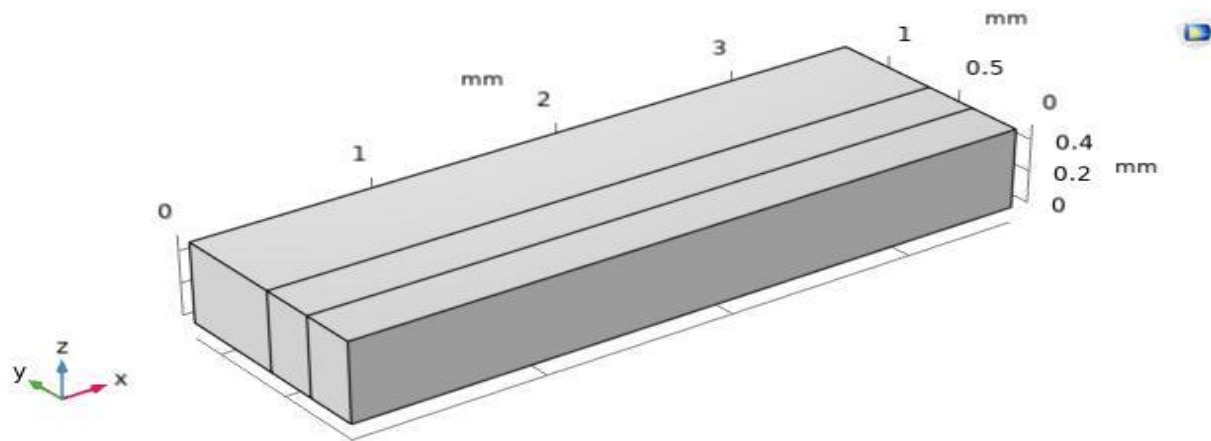


Figure 1- Ti6Al4V Powder Block

b. Parameters used for simulation-

Name	Expression	Unit	Value	Description
Material Parameters-				
T _m	1903	[K]	1903 K	Melting temperature
T _v	3133	[K]	3133 K	Vaporization temperature
L _m	286	[kJ/kg]	2.86E5 J/kg	Latent heat of melting
L _v	9830	[kJ/kg]	9.83E6 J/kg	Latent heat of evaporation
M _v	1.69E-25	[kg/atm]	1.6709E-30 m·s ²	Mass of vapor molecule
alpha1	8.60E-06	[1/K]	8.6E-6 1/K	Thermal expansion coefficient
dsurT	-8.00E-05	[N/m/K]	-8E-5 kg/(s ² ·K)	Temperature derivative of the surface tension
Laser Machining Parameters-				
f	10		10	Number of laser pulses
E _p	0.15	[J]	0.15 J	Pulse energy
E _d	$E_p * f / ((\pi/4) * D^2)$		5.3052E6 J/m ²	Laser Energy density

Pw	10	[ms]	0.01 s	Pulse width
D	0.6	[mm]	6E-4 m	Beam diameter
emi	0.7		0.7	Emissivity
h1	5	[W/m ² /K]	5 W/(m ² ·K)	Heat transfer coefficient
A1	0.25		0.25	Absorptivity
DT	30	[K]	30 K	Half-width of the curve
x0	-D		-6E-4 m	Reference for centre beam
xd	100	[um]	1E-4 m	Standard deviation of the Gaussian laser beam
Vs	2	[mm/s]	0.002 m/s	Scan speed
tstop	(2*D+W1)/Vs		2.4 s	Single pass duration
Ta	293.15	[K]	293.15 K	Ambient temperature
Geometry Block Parameters-				
H1	D*2		0.0012 m	Height of sample
W1	D*6		0.0036 m	Width of sample
D1	D*2		0.0012 m	Depth of sample

Table 1- Parameters used for Simulation

c. Assigning the Major Variables-

Name	Expression	Unit	Description
Ed	$E_p/(P_w * (\pi * 0.25 * D^2))$	W/m ²	Energy Density
G_s	$\exp(-(((x-x_r)^2)/(2 * x_d^2)))$		Gaussian Distribution
Pg	$A_1 * E_d * G_s$	W/m ²	Laser heat source
xr	$x_0 + V_s * t$	m	Laser beam position

Table 2- Major Variables used for Simulation

d. Creating Custom Ti6Al4V material-

Before assigning the layered material, a custom material of Ti6Al4V was made using the material properties as given below-

Piecewise function-

Here T is the Temperature (K) which is the given argument.

Property	Function name	Start (K)	End (K)	Function
Density	rho1	873	1073	$-0.125 * T + 4031.3$
		1073	1323	$-0.8 * T + 5050$
Thermal Conductivity	k	873	1073	$1e-5 * (T^2) - 0.0378 * T + 35.175$
		1073	1323	7.5
Dynamic viscosity	mu	873	1073	0.1
		1073	1323	$1e-3 * (3.2 * \exp(42.2e3/8.314 * T))$
		1323	2000	0.001
Surface Tension	surfT	873	1423	$0.64 - 8.2e-5 * T$

Modulus of Elasticity	E	1073	1423	$407.10-7.3407e-2*T$
Poisson Ratio	nu	873	1323	$0.2644+2e-5*T$
Coefficient of Thermal expansion	alpha_iso	1073	1323	$1e-6*(-0.2306+7.0045e-4*T+5.681e-8*(T^2))$

Table 3- Material Properties for Custom Ti6Al4V

Analytic function-

Heat capacity (Cp) given = $880+((\exp(-((T-1903)^2/30^2)))/(30*\sqrt{\pi}))*286$
 $+(286/1903)*\text{flc2hs}((T-1903),30))+((\exp(-((T-3133)^2/30^2)))/(30*\sqrt{\pi}))*9830$
 $+(9830/3133)*\text{flc2hs}((T-3133),30))$

Settings

Material

▼ Material Contents

▶▶	Property	Variable	Value	Unit	Property group
	Density	rho	rho1(T)	kg/m ³	Basic
	Dynamic viscosity	mu	mu(T)	Pa.s	Basic
	Heat capacity at constant pres...	Cp	Cp(T)	J/(kg.K)	Basic
	Poisson's ratio	nu	nu(T)	1	Basic
	Thermal conductivity	k_iso ;...	k(T)	W/(m...)	Basic
	Young's modulus	E	E(T)	Pa	Basic
	Coefficient of thermal expansi...	alpha_...	alpha_is...	1/K	Basic
	Porosity	epsilon	0.554	1	Porous model

Figure 2- Adding Material Parameter function

e. Assigning Layered Material-

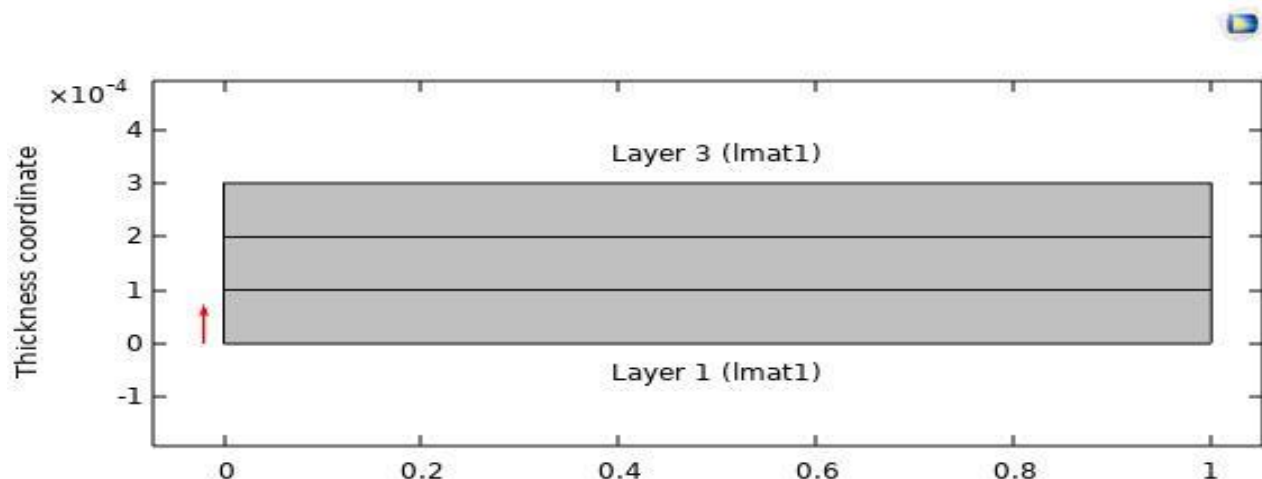


Figure 3- 3 Layer Material

To create a porous structure, Layered Material was assigned. Porosity is also given in Material parameters of Custom Ti6Al4V.

Layer	Material	Rotation (deg)	Thickness	Mesh
Layer 1	Ti6AL4V Custom	0.00	1.00E-04	2
Layer 2	Air	0.00	1.00E-04	2
Layer 3	Ti6AL4V Custom	0.00	1.00E-04	2

Table 4- Layered Material Settings

f. Defining the Laser heat source-

In this simulation, Heat transfer in Solids physics was added. The laser moves in the direction where the heat flux that is applied is traveling on the solid's center layer (Displayed light blue). It is a general inward heat flux. The Gaussian Distribution is the basis for the Laser Heat Source. Pg stands for the Gaussian distribution that the laser beam source uses to travel. As shown in the below figure, the laser beam travels in the middle layer. In simulation, the term "laser" refers to a radiation source that emits radiation and is defined as an energy source. The initial temperature condition is 293.15K. Here Nd-YAG laser parameters is used

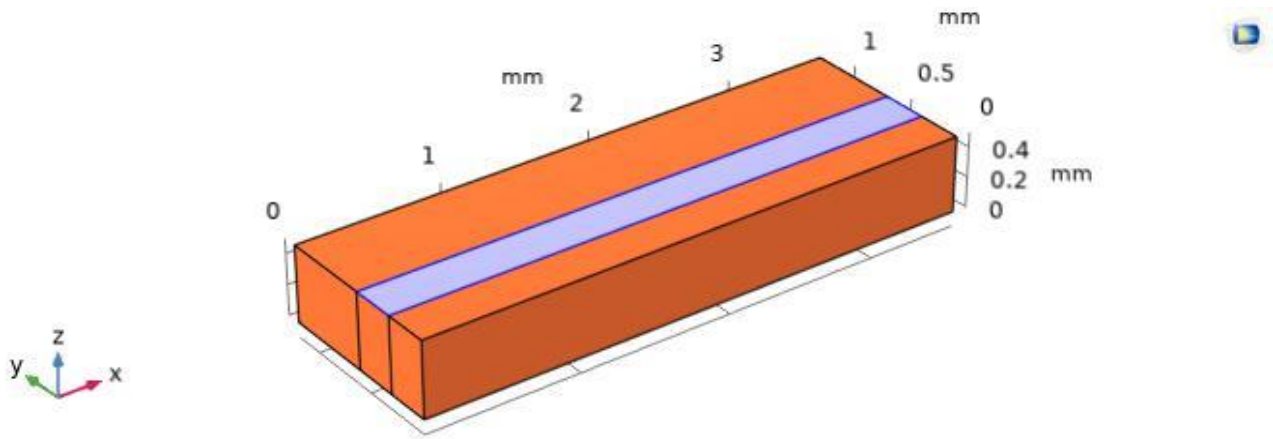


Figure 4- Selecting the center domain for Laser Heat source

The general expression of the Laser heat source is based on Gaussian Distribution and as given below:

$$Pg = A \left(\frac{Ep}{Pw \frac{\pi}{4} D^2} \right) \exp \left[- \left(\frac{(x - xr)^2}{2\phi^2} \right) \right]$$

Here A=Absorptivity, Ep=Pulse Energy, Pw=Pulse Width, D=Beam Diameter, xr=Laser Beam position, ϕ = Standard Deviation of Gaussian Laser Beam.

g. Defining Convection Heat flux-

The Powder block geometry is heated by the laser beam for good bonding between the particles. After the laser has passed through the block it undergoes cooling by 2 processes namely-Convection as well as by radiation. So, it reacts with the atmosphere for cooling. Here we have used h1 as a parameter which is the heat transfer coefficient of 5 W/(m²·K). The Convection is applied to the following domains of the powder block as shown below.

Heat transfer $Q = h_1(T_{ext} - T)$ where $T = 293k$, and T_{ext} depends on laser heat.

h. Defining Radiation-

As discussed above, Radiation is also another factor for heat loss from the geometry. Both Convection and radiation is incorporated into the powder block to create actual conditions that happens after the laser passes through. The surface to ambient radiation is applied to the following domains of the powder block as shown below.

Surface to ambient radiation = $\varepsilon\sigma(T_{ext}^4 - T^4)$ where T where ε =Emissivity, σ = Stefan–Boltzmann constant= $5.67 \times 10^{-8}(\text{W/m}^2 \text{K}^4)$

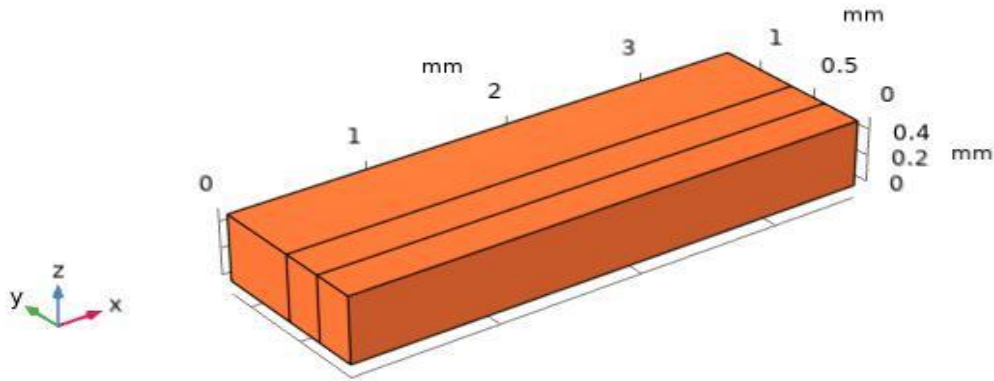


Figure 5- Selecting domains for Convection and Radiation

i. Defining Bed temperature-

Due to laser heating of the powders, the bonding between the particles may not be uniform due to temperature difference among the layers. So, a preheater or a bed temperature can be provided for uniform bonding of the particles in the adjacent layers. The temperature is applied to the following bottom domains of the powder block as shown below.

The temperature that is incorporated here is 950K.

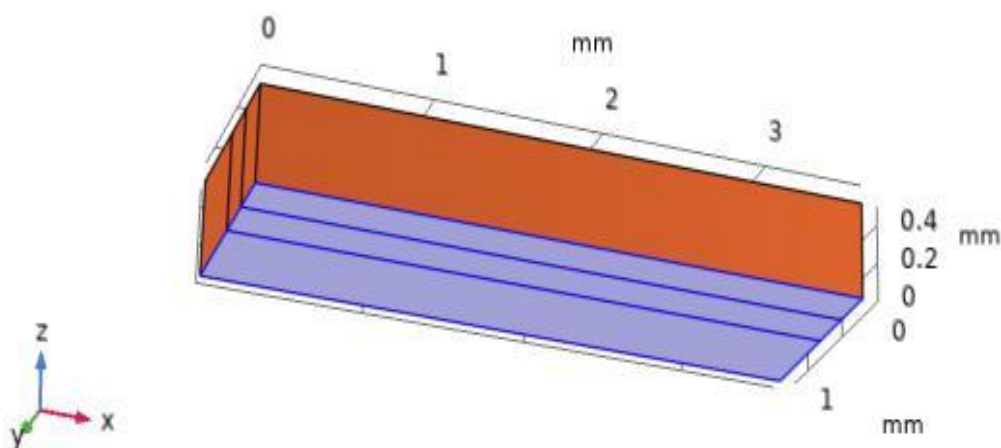


Figure 6- Selecting Bottom domain of the block for bed temperature

j. Setting up Mesh for the powder block-

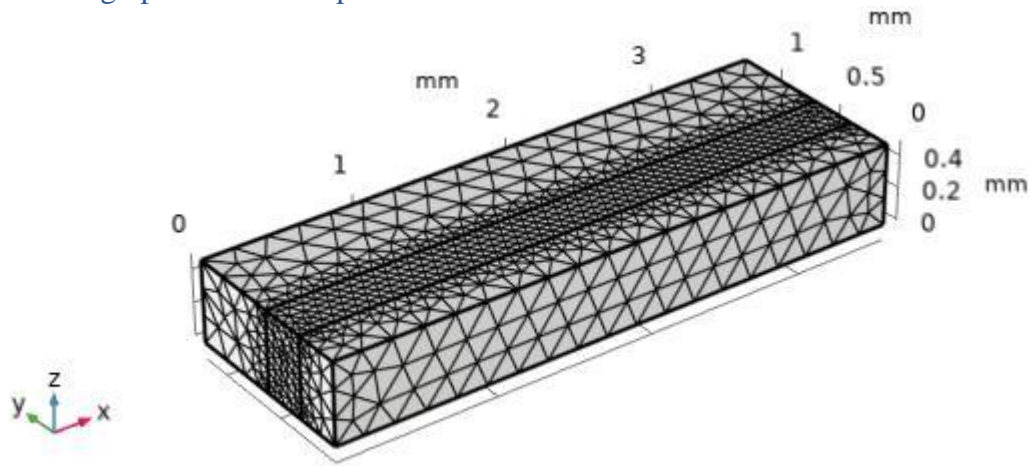


Figure 7- Setting up Mesh for Block

For setting up the mesh for the block, 2 nos. of free tetrahedral type of mesh are taken. One for the center domain for the laser path and the other one for the remaining domains of the block. Both are user-controlled mesh. The first tetrahedral mesh for the center path is given 'extremely fine' and the second tetrahedral mesh for the remaining domains is given 'finer'.

k. Solver Settings-

Here a Time dependent study step is incorporated for the simulation. The time stepping taken by the solver is given Intermediate. Other settings which include are shown below-



Figure 8- Simulation Solver Setting

4. RESULTS AND DISCUSSION-

a. Laser Travel Illustration-

The powder block consists of a moving laser beam, cooling, and heat losses through radiation. As seen in the illustration, a laser beam is moving with respect to time.

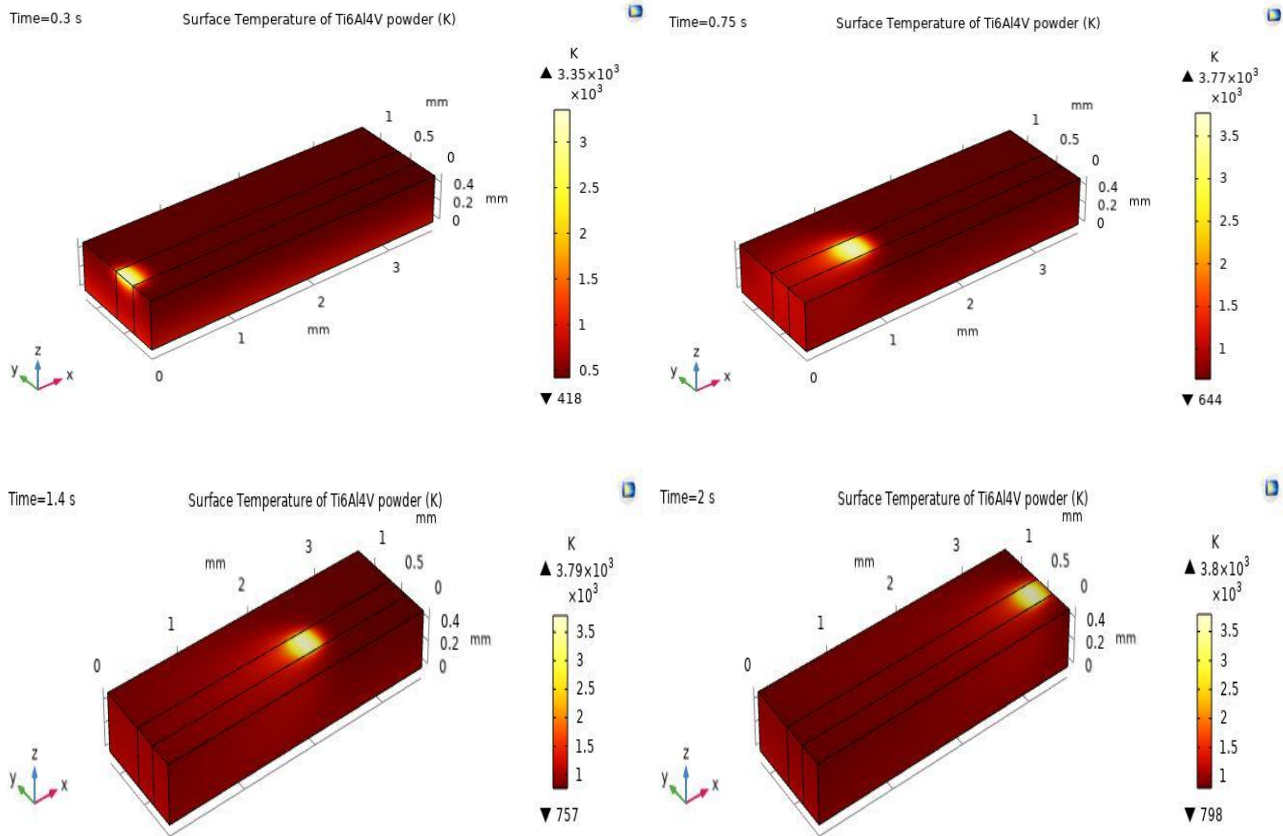


Figure 9- Laser travel on the block at different time interval

b. Defining a cut plane-

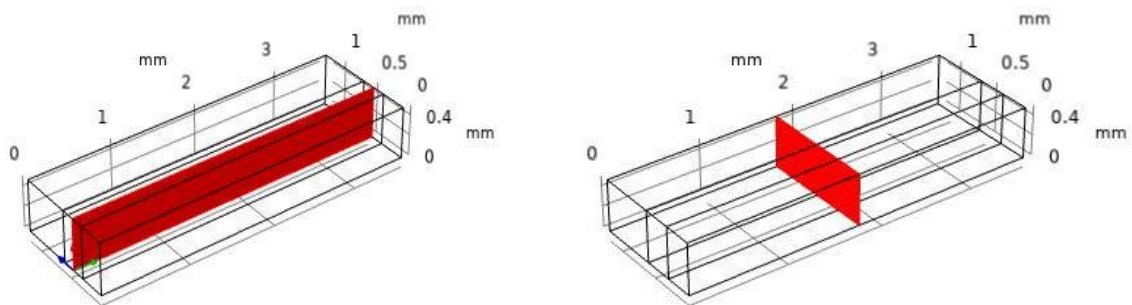


Figure 10- Defining Cut plane ZX (Left) and YZ(Right)

So here 2 cut planes are defined for checking the melt pool temperature distribution at respective cross sections. The first cut plane is ZX plane with Y coordinate 0.45mm. The second cut plane is YZ plane with X coordinate 1.75mm.

c. Melt pool-

- Cut view of the powder block with ZX plane-

- 3D Plot -

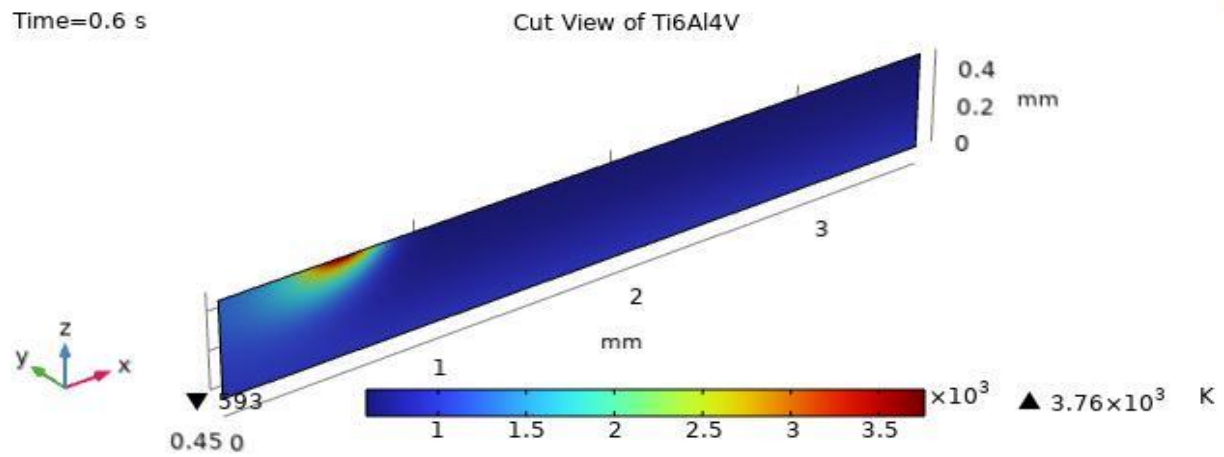


Figure 11- Cut view (ZX) of Ti6Al4V Block in 3D

- 2D plot-

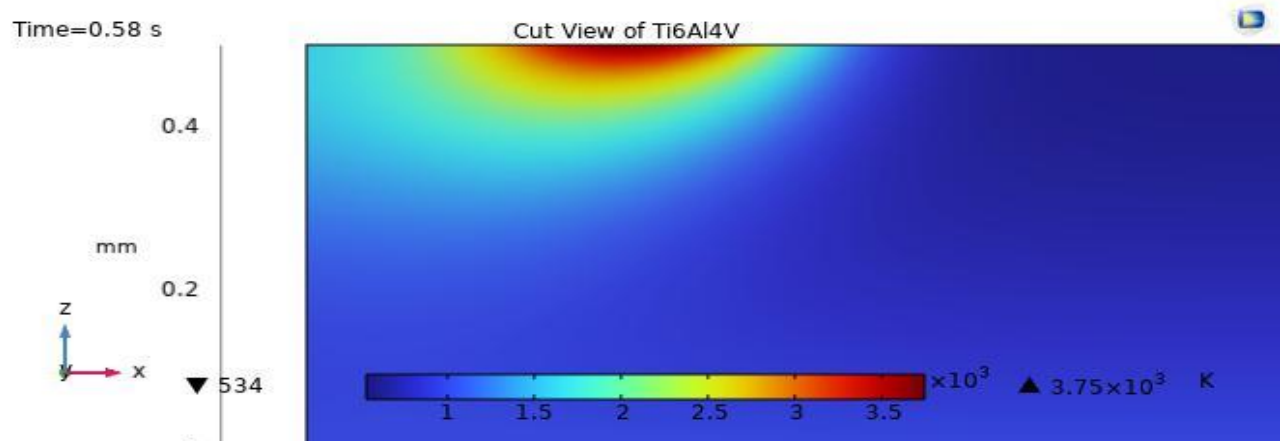
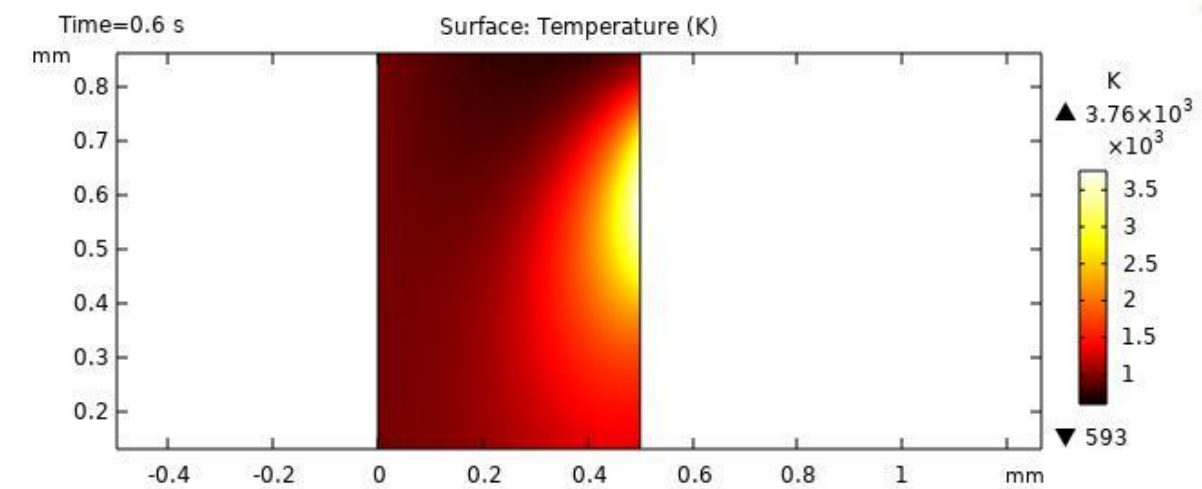


Figure 12- Cut view (ZX) of Ti6Al4V block in 2D displaying Melt pool

-Cut view of the powder block with YZ plane- Shown below is the temperature distribution in the cross section view of the cut plane at different time interval as the laser reaches at that point and leaves.

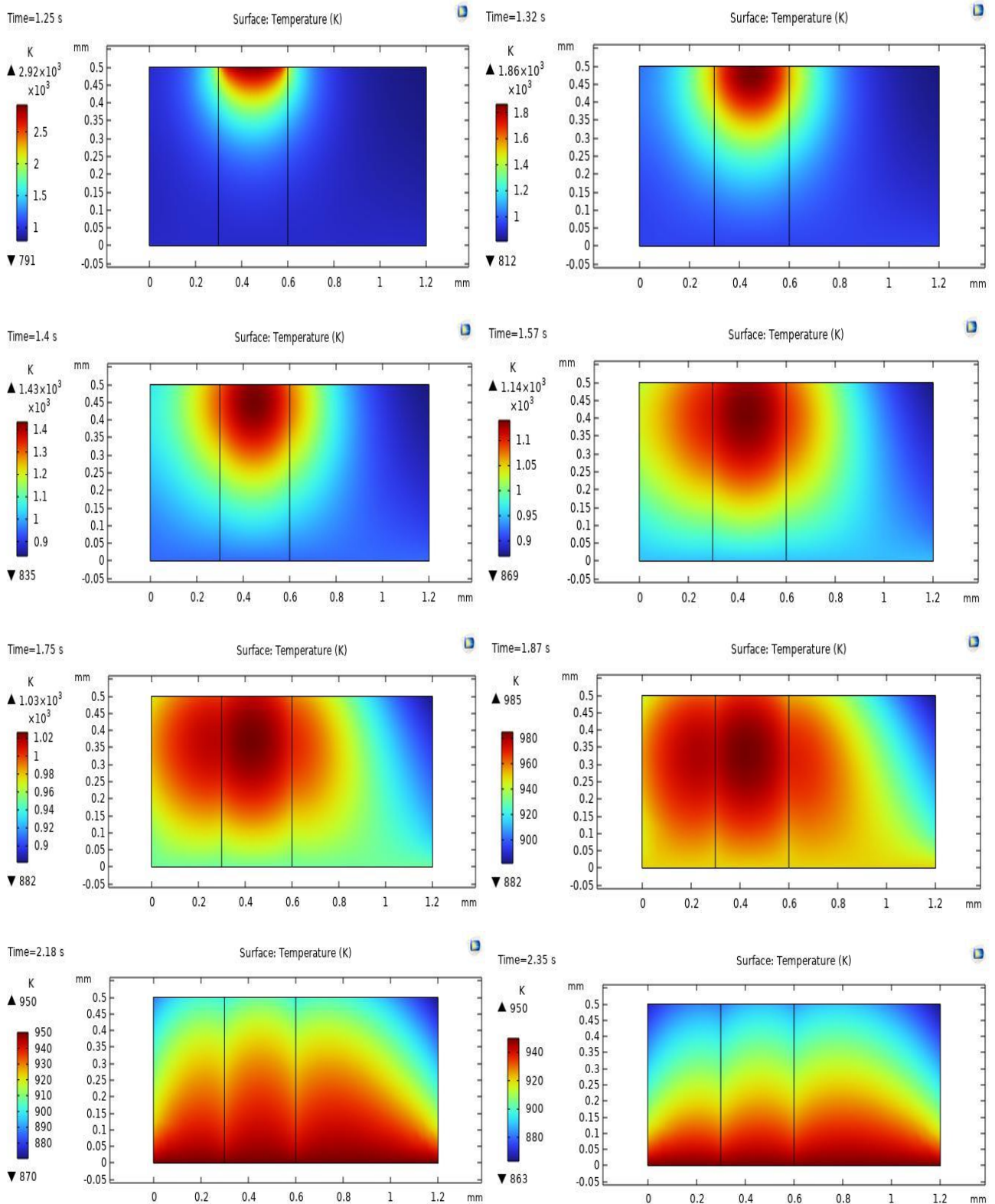


Figure 13- Cut view (YZ) of Ti6Al4V showing melt pool and temperature distribution at different time intervals

As the laser reaches the cross section, the temperature of the block increases gradually and then decreases as the heat distributes and cooling starts at the surface due to convection after the laser crosses the point of cross section.

d. Temperature distribution of powder with Time

The time taken by the laser to travel from one end to the other depends on Laser scan speed as well as the length of the powder block.

- Domain Probe-

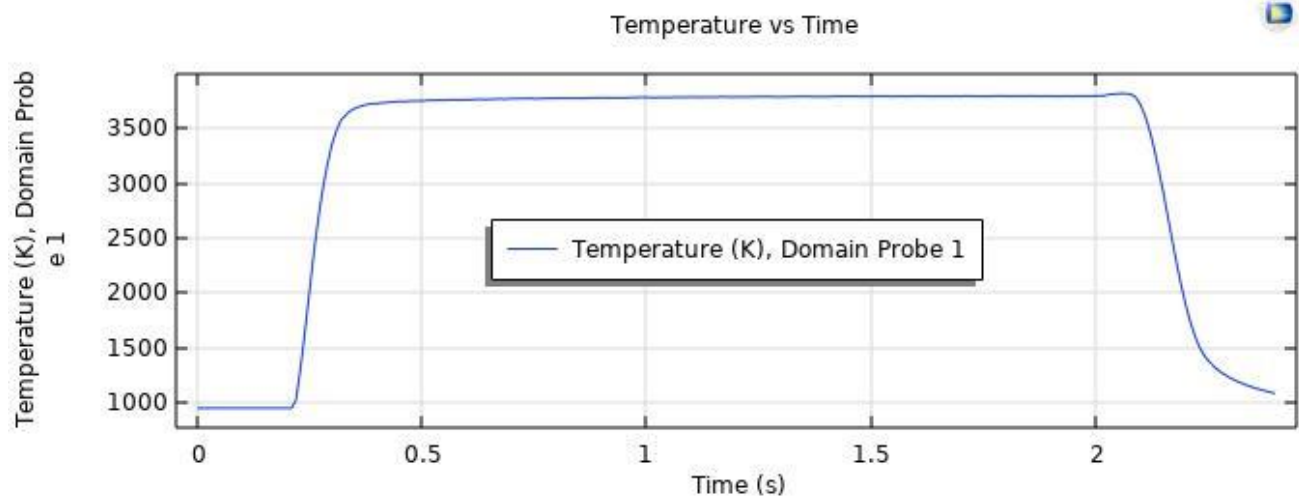


Figure 14- Temperature Distribution with time using Domain probe

Here we have used a domain probe of type-maximum to plot the probe of Temperature vs Time and the domain probe was applied to the entire powder block. According to the probe table and graph- Maximum temperature- 3818.1K at 2.06s.

Minimum temperature observed is 950K at 0.01s.

- Edge probe-

Here an edge probe was applied to one of the laser path edges.

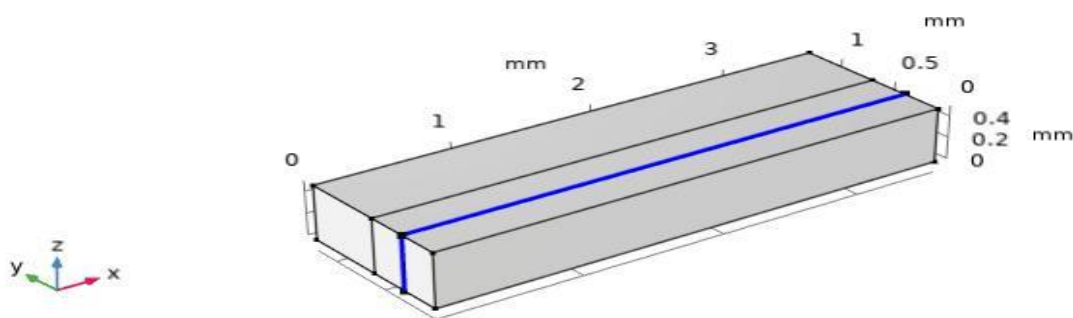


Figure 15- Selecting Laser path edges for Edge probe

The probe plot for the edges is shown below:

Maximum temperature- 2741K at 1.96s

Minimum temperature- 950K at 0.01s

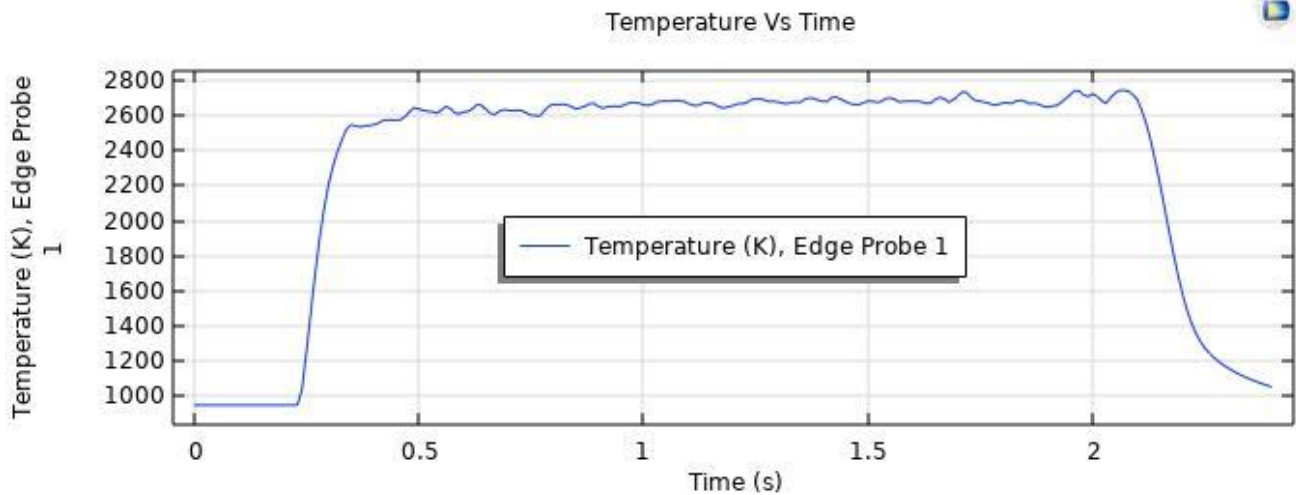


Figure 16- Temperature Distribution with time using Edge probe

- Boundary Point probe-
Here a boundary point probe was selected on the outer edge of the powder bed to check for the temperature changes with time. Coordinates of the point is $(x, y, z) = (1.2824, 0, 0.5)$

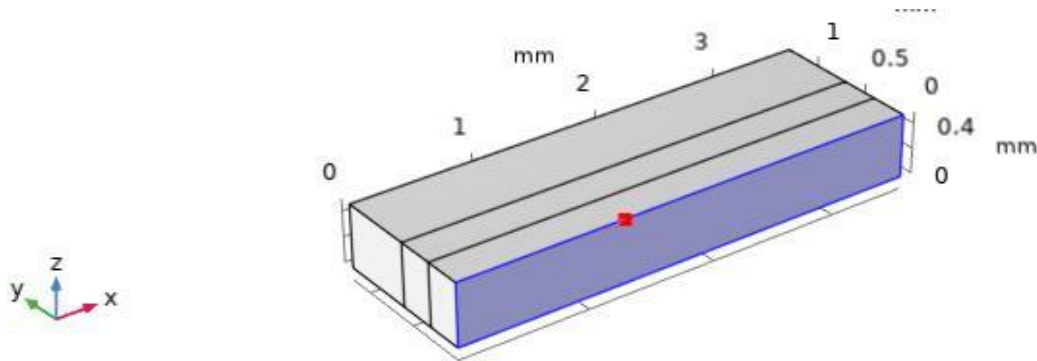


Figure 17- Selecting a point for Boundary point probe

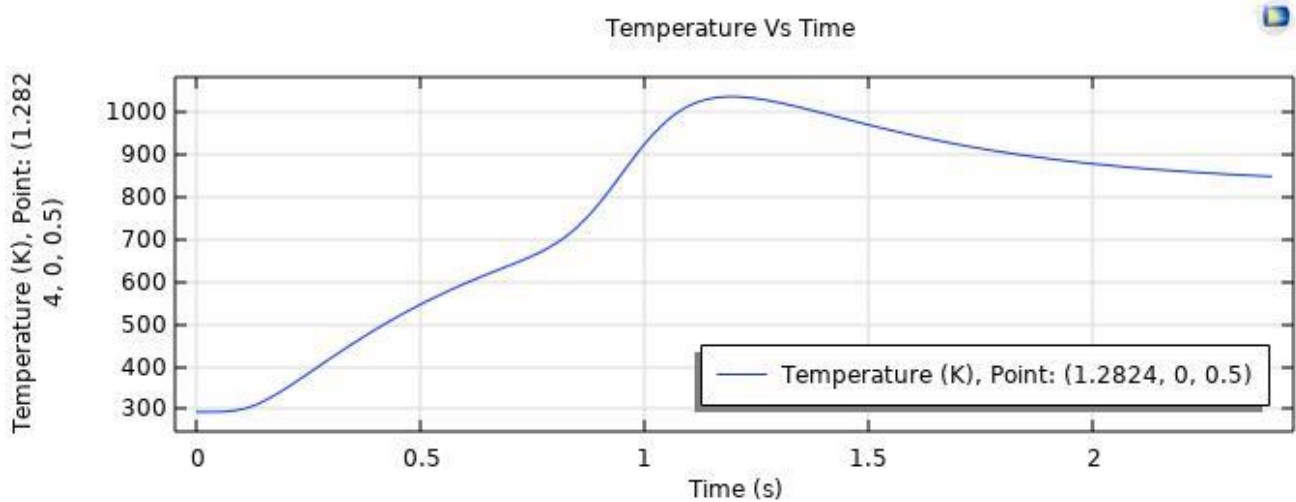


Figure 18- Temperature Distribution with time using Boundary Point probe

Maximum temperature- 1036.4K at 1.2s

Minimum Temperature- 293.15 at 0s

e. Temperature variation in changing Laser Parameters-

- Varying the Laser Scan speed- Here as the Scan speed of the laser is increased; it is observed that the maximum temperature of the edge probe that was selected in the geometry block decreases gradually. Also, the equivalent time corresponding to the Maximum temperature also decreases. The laser energy density remaining constant at 5.3052E6 J/m^2 .

Scan Speed (mm/s)	Max. Temperature (K)	Equivalent Time (s)
2	2741	1.96
2.5	2701	1.66
3	2620	1.4
4	2566	1.04
5	2477.3	0.78
8	2253.7	0.52
10	2121	0.42

Table 5- Temperature Variation with Varying Laser Scan Speed

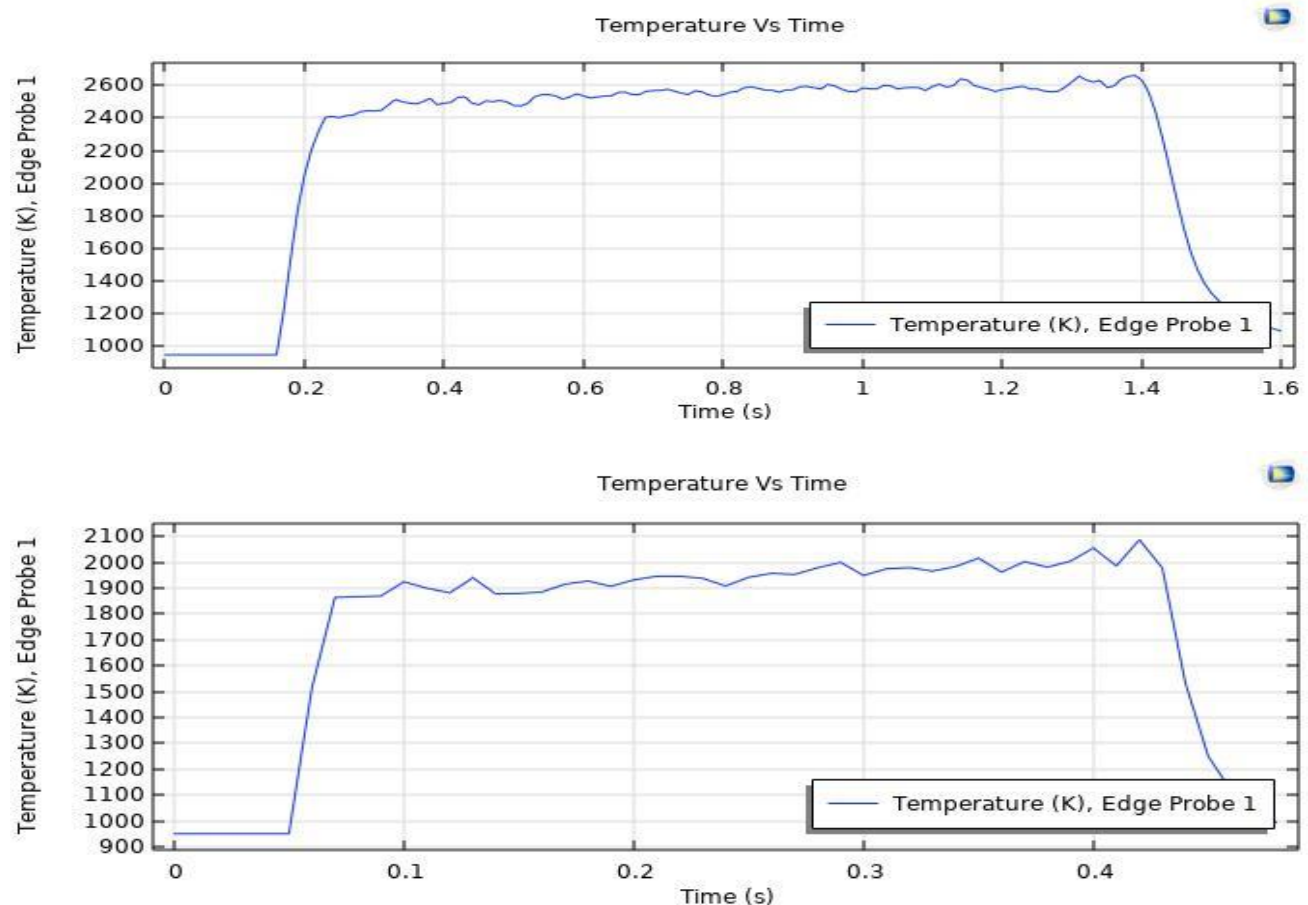


Figure 19- Temperature Variation by varying the Scan speed: (a) $V_s = 3\text{mm/s}$, (b) $V_s = 10\text{mm/s}$

- Varying the Laser Energy density- Here as the Energy density is increased; the Laser heat source also increases. This results in increase of the maximum temperature of the edge probe that is applied in the geometry as shown in the below table. Here the Scan speed is kept constant at 2mm/s.

Energy Density (J/m ²)	Max. Temperature (K)	Equivalent Time (s)
5.31E+06	2741	1.96
8.84E+06	3251.7	2.06
1.24E+07	3612.1	1.72
1.59E+07	3945	1.96
2.12E+07	4300.4	1.96

Table 6- Temperature Variation with Varying Laser Energy Density

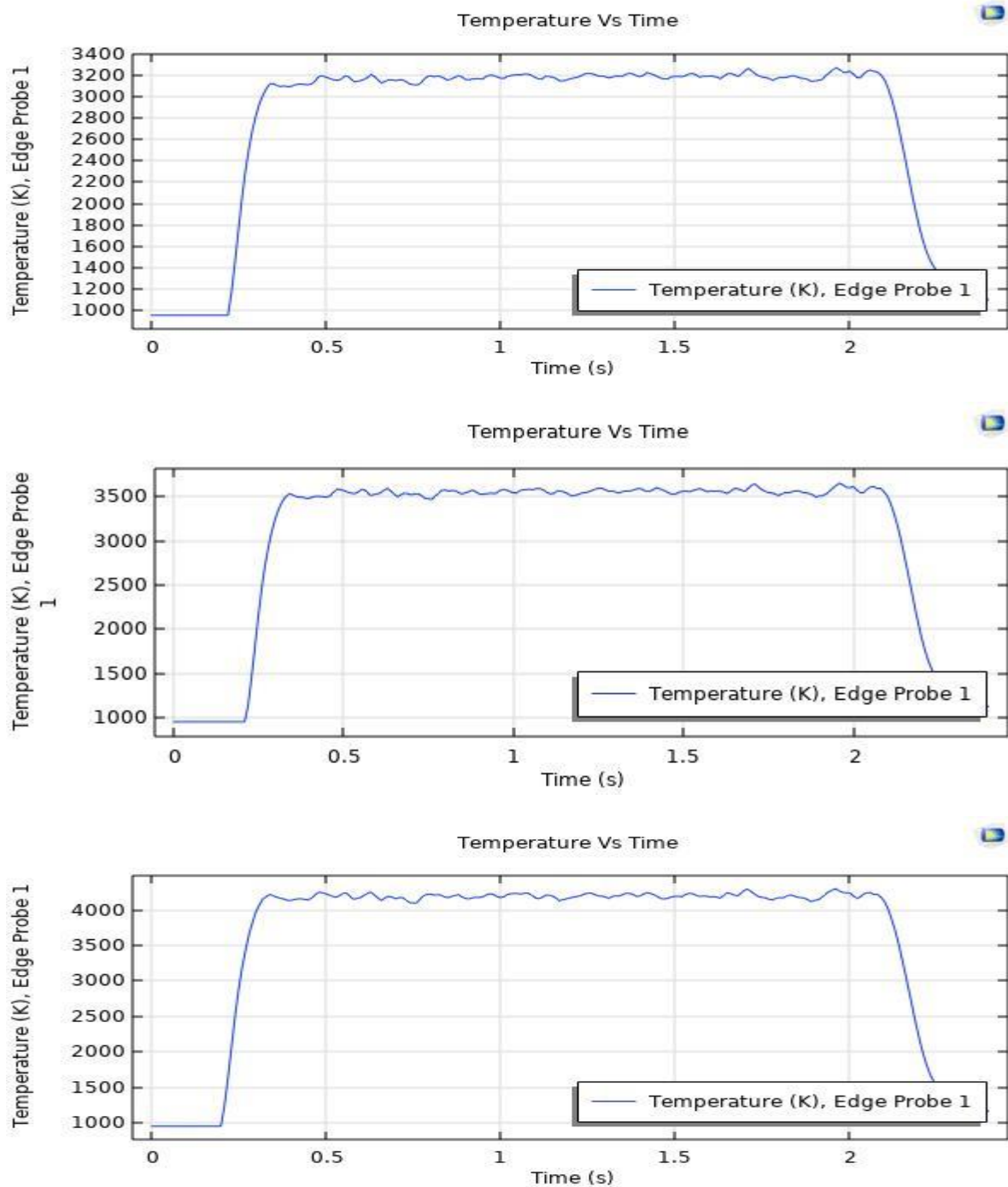


Figure 20- Temperature Variation by Varying Energy Density: (a) $Ed=8.84E+06$, (b) $Ed=1.24E+07$, (c) $Ed=2.12E+07$

5. CONCLUSION-

In this report, the melting pool and temperature distribution of Ti6Al4V particles with time is studied. The maximum and operating temperatures at various regions of the powder bed were examined when modeling the simulation of the SLM process. The temperature distribution over time was also examined by adjusting the Laser scan speed and Energy density. The selective laser melting procedure revealed the following observations: temperature increases with increasing laser energy density and lowers with increasing scan speed.

6. REFERENCES-

- Liu Cao (2019) Study on the numerical simulation of laying powder for the selective laser melting process. doi:10.1007/s00170-019-04440-4
- Hitesh D Vora, Soundarapandian Santhanakrishnan (2013) One-dimensional multipulse laser machining of structural alumina: evolution of surface topography. Int J Adv Manuf Technol. doi:10.1007/s00170-012-4709-8
- Anil Kumar Singla a, Mainak Banerjee, Aman Sharma, Jagtar Singh, Anuj Bansal (2021) Selective laser melting of Ti6Al4V alloy: Process parameters, defects and post-treatments. doi:10.1016/j.jmapro.2021.01.009
- Haijun Gong, Hengfeng Gu, Kai Zeng, J.J.S. Dilip, Deepankar Pal, Brent Stucker (2015) Melt Pool Characterization for Selective Laser Melting of Ti-6Al-4V Pre-alloyed Powder. <https://www.researchgate.net/publication/280114580>